The GTPase SPAG-1 orchestrates meiotic program by dictating meiotic resumption and cytoskeleton architecture in mouse oocytes

Chunjie Huang, Di Wu, Faheem Ahmed Khan, Xiaofei Jiao, Kaifeng Guan, and Lijun Huo*
Key Laboratory of Agricultural Animal Genetics, Breeding and Reproduction, Education Ministry of China, College of Animal Science and Technology, Huazhong Agricultural University, Wuhan 430070, China

ABSTRACT **In mammals, a finite population of oocytes is generated during embryogenesis, and proper oocyte meiotic divisions are crucial for fertility. Sperm-associated antigen 1 (SPAG-1) has been implicated in infertility and tumorigenesis; however, its relevance in cell cycle programs remains rudimentary. Here we explore a novel role of SPAG-1 during oocyte meiotic progression. SPAG-1 associated with meiotic spindles and its depletion severely compromised M-phase entry (germinal vesicle breakdown [GVBD]) and polar body extrusion. The GVBD defect observed was due to an increase in intraoocyte cAMP abundance and decrease in ATP production, as confirmed by the activation of AMP-dependent kinase (AMPK). SPAG-1 RNA interference (RNAi)–elicited defective spindle morphogenesis was evidenced by the dysfunction of γ-tubulin, which resulted from substantially reduced phosphorylation of MAPK and irregularly dispersed distribution of phospho-MAPK around spindles instead of concentration at spindle poles. Significantly, actin expression abruptly decreased and formation of cortical granule–free domains, actin caps, and contractile ring disrupted by SPAG-1 RNAi. In addition, the spindle assembly checkpoint remained functional upon SPAG-1 depletion. The findings broaden our knowledge of SPAG-1, showing that it exerts a role in oocyte meiotic execution via its involvement in AMPK and MAPK signaling pathways.**

Monitoring Editor
Jonathan Chernoff
Fox Chase Cancer Center

Received: Feb 29, 2016
Revised: Mar 29, 2016
Accepted: Mar 31, 2016

INTRODUCTION

The female reproductive potential is expressed through a fixed pool of oocytes produced by the mammalian ovary during embryogenesis through the entire reproductive lifespan (Yu *et al.*, 2013; Qiao and Li, 2014). More significantly, the generation of a haploid egg through meiotic divisions of mammalian oocytes, especially maternal aged oocytes, is an error-prone event that puts oocytes at the risk of aneuploidy (Clift and Schuh, 2015; Pfender *et al.*, 2015; Saloojee and Coovadia, 2015). When an aneuploid egg is inherited by an embryo, miscarriage or chromosomally abnormal pregnancies occur (Kouznetsova *et al.*, 2007; Nagaoka *et al.*, 2012; Holubcová *et al.*, 2015)—further highlighting the importance of understanding the biology of mammalian oocytes. The mammalian oocyte undergoes two consecutive asymmetric divisions, meiosis I and meiosis II, without an intervening DNA replication, ultimately producing a highly polarized haploid gamete, the egg, which preserves maternal resources for fertilization and subsequent early embryogenesis (Schuh and Ellenberg, 2007; Dumont and Desai, 2012; Almonacid *et al.*, 2014). However, our knowledge of oocyte meiosis at the molecular level remains elusive.

Oocyte meiosis is reinitiated (marked by M-phase entry) after it experiences a protracted diplotene stage of meiotic prophase I (germinal vesicle stage [GV]) by intraoocyte cAMP through cyclin-CDK activation accompanied by drop in cAMP concentration characterized by germinal vesicle breakdown (GVBD; Zhang and Xia, 2012; Gui and Homer, 2013; Holt *et al.*, 2013; Wang *et al.*, 2015). After GVBD, centrally positioned meiotic spindles form and migrate to the cortex of oocytes in an actin-dependent manner (Almonacid *et al.*, 2014). Another feature of the oocyte is a lack of centrosomes and their associated astral microtubules, in which

This article was published online ahead of print in MBoC in Press (http://www.molbiolcell.org/cgi/doi/10.1091/mbc.E16-02-0132) on April 6, 2016.

*Address correspondence to: Lijun Huo (lijunhuo@yahoo.com).

Abbreviations used: CGFD, cortical granule–free domain; GVBD, germinal vesicle breakdown; MTOC, microtubule-organizing center; SAC, spindle assembly checkpoint; SPAG-1, sperm-associated antigen 1.

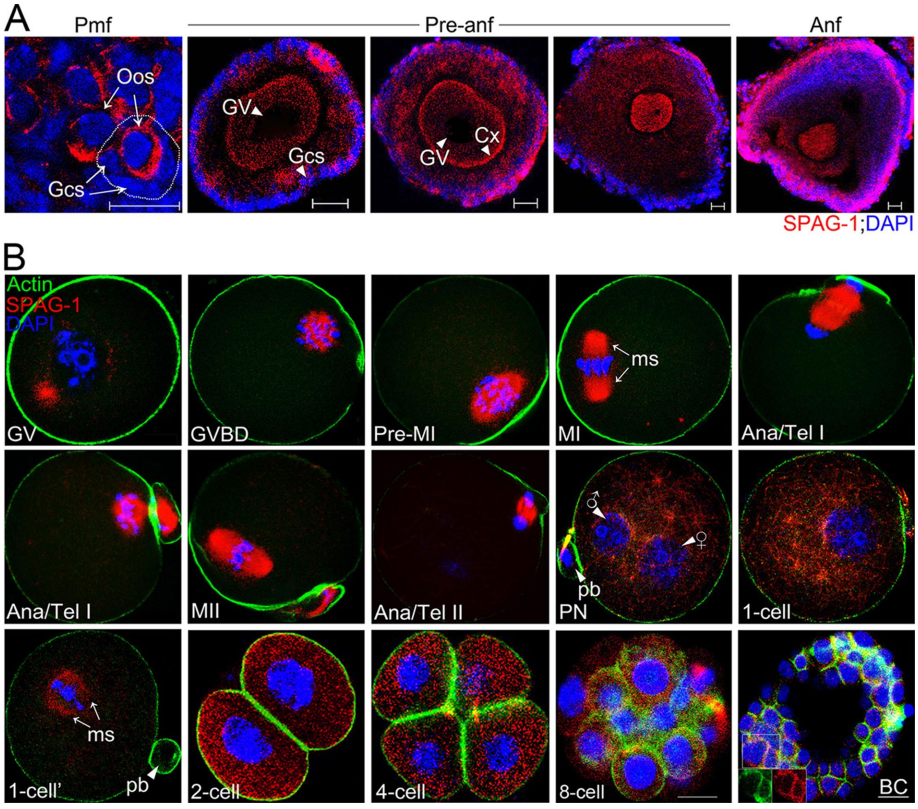

FIGURE 1: SPAG-1 in female gametogenesis and early embryogenesis. (A) SPAG-1 localization during folliculogenesis. Follicles at a range of developmental stages (indicated at the top) were immunostained with anti-SPAG-1 (red) and 4′,6-diamidino-2-phenylindole (DAPI; blue). Scale bar, 10 μm. (B) SPAG-1 localization during oocyte in vivo meiotic maturation and early embryogenesis. Oocytes or embryos at indicated stages were prepared for immunostaining with anti-SPAG-1 (red) antibody and phalloidin (F-actin; green). DNA (blue) was visualized by DAPI staining. The completion of oocyte meiosis II is triggered by fertilization and followed by early zygotic divisions. Female and male pronuclei are indicated by gender symbols. Enlargements are shown boxed in the merged images. Scale bar, 20 μm. Ana/Tel I/II, anaphase/telophase of meiosis I/II; Anf, antral follicle; BC, blastocyst; Cx, cortex; Gcs, granulosa cells; ms, meiotic or meiotic spindles; Oos, oocytes; pb, first polar body; Pmf, primordial follicle; PN, pronuclear; Pre-anf, preantral follicle.

spindle morphogenesis is directed by a proteinaceous structure called the microtubule-organizing center (MTOC), comprising γ-tubulin and additional microtubule nucleators (Schuh and Ellenberg, 2007; Sun *et al.*, 2011; Dumont and Desai, 2012; Han *et al.*, 2015; Huang *et al.*, 2015). The asymmetrical inheritance of oocyte meiosis is accompanied by profound changes in cytoskeletal remodeling, which include spindle rotation and migration, spindle cortical anchoring, and cleavage furrow ingression (Almonacid *et al.*, 2014). Furthermore, actin reassembles to form the actin cap, cortical granules redistribute to form a cortical granule–free domain (CGFD), and microvilli disappear in the cortical region overlying the spindles (Sun *et al.*, 2011; Dehapiot *et al.*, 2013; Almonacid *et al.*, 2014). To guarantee faithful chromosome segregation, chromosomes aligned at the metaphase plate need to establish bioriented attachment with spindle microtubules under proper tension before anaphase is allowed to proceed by satisfying the spindle assembly checkpoint (SAC; Kouznetsova *et al.*, 2007; Nagaoka *et al.*, 2012; Yun *et al.*, 2014; Holubcová *et al.*, 2015). Subsequently completion of meiosis I, signified by expelling of the first polar body, is executed by cytokinesis, which constricts the oocyte at the cleavage plane into two parts (Sun *et al.*, 2011; Holubcová *et al.*, 2015; Huang *et al.*, 2015).

The small-GTPase family is abundant and highly conserved in eukaryotic cells, and one of the extensively established small GTPases, Ran, has been implicated in myriad cellular events, including nucleocytoplasmic trafficking, spindle morphogenesis, cortical reorganization, and nuclear envelope architecture (Clarke and Zhang, 2001; Deng *et al.*, 2007; Serio *et al.*, 2011; Yi *et al.*, 2011). Like Ran, Sperm-associated antigen 1 (SPAG-1) possesses both GTP-binding and GTPase activity (Lin *et al.*, 2001; Neesse *et al.*, 2007). SPAG-1 predominantly localizes to the neck and midpiece of pachytene primary spermatocytes and was found to be involved in female infertility (Lin *et al.*, 2001; Liu *et al.*, 2006; Knowles *et al.*, 2013). Further studies determined the association of SPAG-1 with pancreatic tumorigenesis and the potential involvement of SPAG-1 in AMP-dependent kinase (AMPK), mitogen-activated protein kinase (MAPK), and protein kinase C (PKC) signaling cascades (Lin *et al.*, 2001; Neesse *et al.*, 2007; Knowles *et al.*, 2013). Despite the significance of these pathways in oocyte meiotic resumption, cytoskeletal organization and cytokinesis have been acknowledged by many studies (Chen *et al.*, 2009; Sun *et al.*, 2011; Holt *et al.*, 2013; Ya and Downs, 2013; Kotak *et al.*, 2014; Zhang *et al.*, 2015); however, it is uncertain whether SPAG-1 contributes to the oocyte developmental program and, if it does, what underlying mechanisms might be involved.

In this study, we explored the function of SPAG-1 by examining its localization and expression during mouse oocyte meiosis both in vivo and in vitro. In addition, RNA interference–mediated silencing of SPAG-1 allows us to decipher a novel role of SPAG-1 in meiotic programs by orchestrating meiotic progression and cytoskeletal architecture via its potential involvement in AMPK and MAPK signaling pathways. Our findings indicate that SPAG-1 GTPase plays a role in mammalian gametogenesis and fertility.

RESULTS

Subcellular localization of SPAG-1 during female gametogenesis and early embryogenesis

SPAG-1 localizes to the neck and midpiece of pachytene primary spermatocytes; however, its dynamics during oogenesis and early embryogenesis has not been addressed. We investigated the localization of SPAG-1 in the course of oogenesis and early embryogenesis by immunostaining. Mammalian oocytes enter into meiosis and experience a protracted diplotene stage of prophase I with a growth phase during folliculogenesis. In primordial follicles, SPAG-1 localized to the cytoplasm of primary oocytes. During the developmental stage of preantral follicle, SPAG-1 remained localized in the cytoplasm of oocytes, with an apparent accumulation in the cell cortex. However, SPAG-1 expression was diffused across the cytoplasm of GV-stage oocytes in antral follicles, implying that SPAG-1 might be involved in oocyte growth during folliculogenesis (Figure 1A).

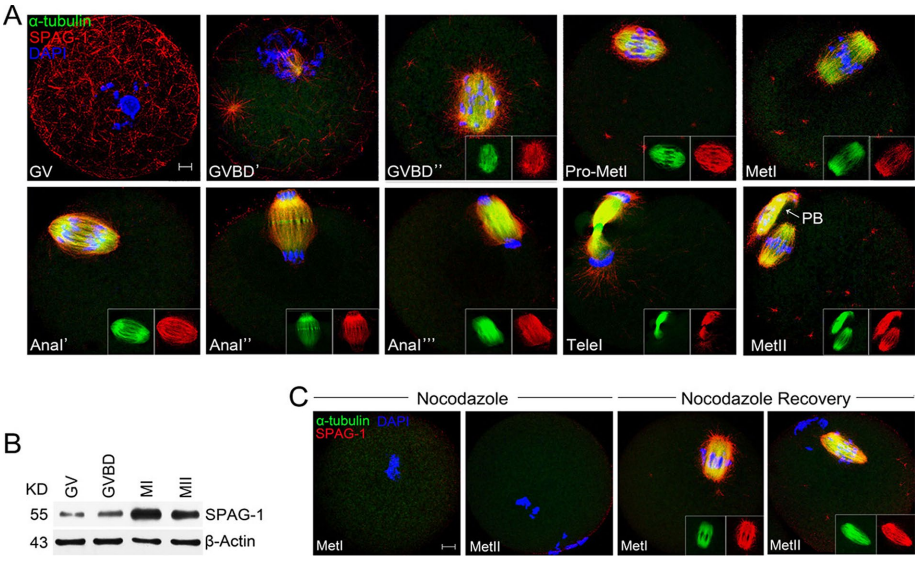

FIGURE 2: SPAG-1 dynamics in mouse oocytes during in vitro meiotic maturation. (A) Cellular localization of SPAG-1 detected by immunofluorescence analysis. Oocytes at indicated stages were immunostained for SPAG-1 (red), microtubule (green; α-tubulin), and DNA (blue). (B) Total cellular lysates from oocytes at corresponding stages as indicated along the top were prepared for IB. (C) Confocal *Z*-projections of oocytes at MI or MII stage before or after treatment with nocodazole were stained as in A. Enlargements of regions corresponding to the spindle are shown to clarify the association of SPAG-1 with the spindle. Scale bar, 10 μm.

Oocyte meiosis resumes at the final phase of folliculogenesis, followed by the completion of meiosis I (marked by first polar body extrusion). To assess the expression pattern of SPAG-1 during in vivo oocyte meiotic maturation, we prepared oocytes at specific stage for immunofluorescence analysis. At the GV stage, SPAG-1 accumulated as cytoplasmic dots around the nuclei, with some foci attached to the GV. After GVBD, SPAG-1 was enriched in the close proximity of chromosomes and tightly associated with the dynamics of meiotic spindles until metaphase II, at which oocytes encountered the second meiotic arrest (Figure 1B).

The completion of meiosis II (marked by expelling the second polar body) can be triggered by sperm penetration followed by the formation of female and male pronuclei and early embryogenesis. SPAG-1 maintained its microtubule-associated localization during the final steps of meiosis II and evenly dispersed into the cytoplasm of pronucleus-stage zygotes, with discernible signals in the remnant spindles of the second polar body. After the fusion of female and male pronuclei, the zygote then initiates the mitotic division program, and SPAG-1 reassembles to overlap with the mitotic spindles in the one-cell embryo. During mitotic divisions of zygotes in early embryogenesis, SPAG-1 predominantly yielded a diffused cytoplasmic signal in interphase cells and a spindle-associated signal in dividing cells (Figure 1B and Supplemental Figure S1).

Dynamics of expression pattern of SPAG-1 during oocyte in vitro meiotic maturation

To explore the possible role of SPAG-1 in mammalian oocyte meiotic program, we next examined the localization and expression patterns of SPAG-1 during oocyte in vitro meiotic maturation. In GV oocytes, SPAG-1 exhibited unexpected cytoskeleton-like filamentous structures diffused into cytoplasm. Soon after GVBD, microtubules were organized to form bipolar meiotic spindles, and SPAG-1 signals were reassembled into astral structures in the vicinity of the scattered chromosomes, with numerous filaments in the cytoplasm. After that, SPAG-1 dynamically associated with meiotic spindles and the peripheral region surrounding spindles. Significantly, some foci for SPAG-1 in the areas devoid of microtubule structures were visible from late GVBD to the metaphase II (MII stage), which is reminiscent of the expression pattern of SPAG-1 in the in vivo meiotic process (Figure 2A). Furthermore, our quantitative Western blot data showed that the native expression level of SPAG-1 increased from GVBD to the metaphase I (MI) stage and then slightly declined in the MII stage (Figure 2B).

Accumulation of SPAG-1 to meiotic spindles might depend on the integrity of microtubules, because upon treatment of MI and MII oocytes with the reversible microtubule depolymerizing-agent nocodazole, which completely abrogates microtubules, SPAG-1 disassociated from spindles, with diffuse signals in cytoplasm. However, when the treated oocytes were liberated from nocodazole and recovered in fresh medium, SPAG-1 relocalized to the reforming spindle apparatus, further confirming the association of SPAG-1 with meiotic spindles (Figure 2C). Based on the dynamic spatiotemporal changes in cellular localization of SPAG-1 during meiosis, SPAG-1 can be seen as a novel microtubule-associated protein that potentially dictates oocyte meiotic progression.

Depletion of SPAG-1 compromises oocyte meiotic progression

To explore the relevance of SPAG-1 in oocyte meiotic progression, we repressed SPAG-1 native expression by RNA interference (RNAi), which yielded ~70% depletion of SPAG-1 proteins (Figure 3A). After RNAi, oocytes were continuously cultured up to 14 h for maturation assessment. The progression through G2/M (marked by GVBD) was dramatically compromised in SPAG-1–depleted oocytes compared with that in the control group even after 3 h in culture (13.6 vs. 92.8%, $p < 0.001$; Figure 3B). Moreover, compared with control oocytes, SPAG-1–silenced oocytes barely executed the first polar body extrusion after 14 h in culture (8.0 vs. 67.4%, $p < 0.001$; Figure 2C) with >60% of oocytes still significantly arrested at the GV stage ($p < 0.001$; Figure 2C). Taken together, the results show that SPAG-1 is required for oocyte release from prophase arrest and expulsion of the polar body.

Silencing of SPAG-1 disrupts energy homeostasis in oocytes

ATP, a product of cellular energy metabolism, has been recognized as a marker of oocyte quality and subsequent developmental competence (Gu *et al.*, 2015; Wu *et al.*, 2015). Penetration of an oocyte to complete fertilization is a highly energy consuming process for sperm, and immunoneutralization of SPAG-1 disrupts the motility of cells, implying possible involvement of SPAG-1 in energy metabolism. To this end, we assessed ATP concentration. As expected, SPAG-1 RNAi yielded a precipitous reduction of ATP level, as indicated by the relative luminescence intensity (Figure 4A). Further, an appreciable increase in AMP production was also observed, as indirectly reflected by the activation of AMP-dependent kinase (AMPK; Figure 4B). Intra-oocyte cAMP orchestrates protracted meiotic prophase I (GV) stage arrest during oocyte in vitro maturation. To examine whether the pronounced prophase arrest in SPAG-1–depleted

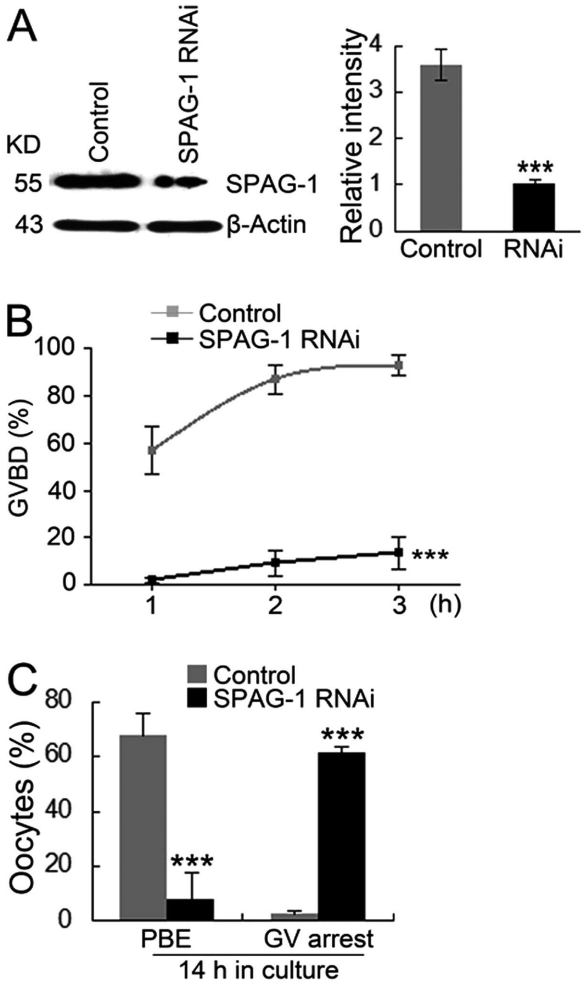

FIGURE 3: Depletion of SPAG-1 interferes with M-phase entry and first polar body extrusion. Live oocytes microinjected with control siRNA or SPAG-1 siRNA were maintained in M2 medium containing 50 μM IBXM for 24 h and then released into fresh M16 medium for continuous culturing. (A) Knockdown efficiency of SPAG-1 RNAi was validated by IB. (B) The kinetics of GVBD was scored at different time points as indicated. (C) Quantification of polar body extrusion rate and oocytes arrested at the GV stage after continuous culture for 14 h. We analyzed 237 oocytes in control and 191 oocytes in SPAG-1 RNAi. Data are presented as mean ± SEM. ***$p < 0.001$.

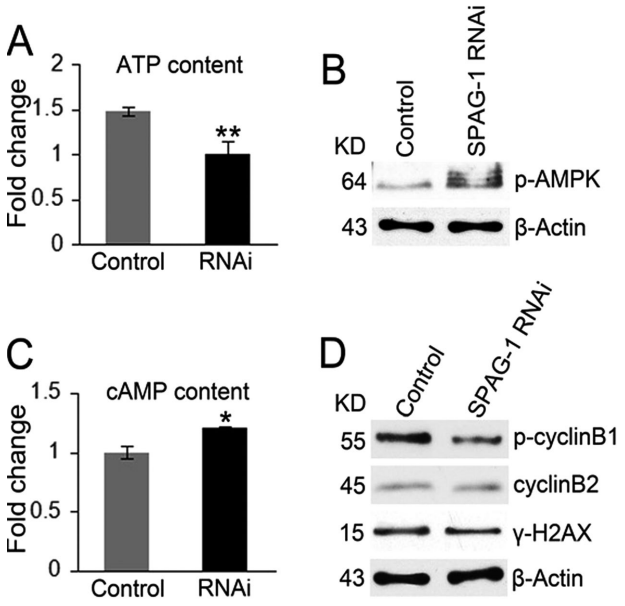

FIGURE 4: Silencing of SPAG-1 perturbs energy metabolism in oocytes. Live GV oocytes injected with control siRNA or SPAG-1 siRNA were prepared for luciferase or IB assay. (A) Content of ATP was measured by luciferase assay. (B) Expression of phosphorylated AMPK was assessed by IB assay. Note that the activation of AMPK indirectly indicates the elevated level of AMP. (C) Concentration of cAMP was measured as in A. (D) Expression of phosphorylated cyclin B1 and other M-phase entry–related regulators as indicated at the right side were analyzed. Data from at least three independent experiments are presented as mean ± SEM. *$p < 0.05$ and **$p < 0.01$.

oocytes could be partially interpreted in terms of an elevation in cAMP concentration, we evaluated the cAMP level. Of note, cAMP concentration in SPAG-1–silenced oocytes was indeed significantly higher than that in control oocytes, as revealed by the lower luminescence intensity of ATP (Figure 4C).

Accompanied by a reduction of cAMP, oocyte meiosis resumption is triggered by the accumulation and activation of cyclin-CDK (Gui and Homer, 2013; Holt *et al.*, 2013). Soon before M-phase onset, cyclin B1 is phosphorylated and translocated to the nucleus to modulate G2/M transition. Of note, the phosphorylation of cyclin B1 in SPAG-1–silenced oocytes was significantly attenuated (Figure 4D). Cyclin B2 is a newly elucidated determinant of meiosis initiation in mammal oocytes, and phosphorylation of H2A.X is required for DNA damage–mediated cell cycle arrest. However, expression of neither cyclin B2 nor phospho-H2A.X was affected by SPAG-1 RNAi (Figure 4D). In addition, we found that extensive acetylation in mouse oocytes induced by sodium butyrate treatment ablated GVBD, which phenocopied our result (unpublished data). Nevertheless, the acetylation on H3K9 was comparable in both groups (Supplemental Figure S2). We propose that SPAG-1, partially by facilitating energy metabolism and phosphorylation of cyclin B1, dictates the execution of M- phase entry.

SPAG-1 facilitates MAPK phosphorylation to modulate meiotic spindle morphogenesis

We observed that, in SPAG-1–silenced oocytes, polar body extrusion was tremendously reduced, prompting us to investigate the consequences of SPAG-1 depletion beyond M-phase entry. We analyzed spindle morphology in oocytes. After 14 h in culture, in sharp contrast to control oocytes, which extruded polar bodies with typical barrel-shaped spindles arrested at the MII stage, SPAG-1–depleted oocytes displayed a faint staining signal of α-tubulin or remnant spindles dispersed across the chromosomes, and the presence of aberrant spindles was observed in almost all SPAG-1–depleted oocytes (Figure 5, A and B). Moreover, cell cycle analysis of the unmatured oocytes revealed that SPAG-1–silenced oocytes were significantly arrested at GVBD or the pro-MI stage (Figure 5C). The defect in spindle formation might arise from a failure of microtubules to assemble into bipolar spindles rather than from the instability of microtubules, because the expression of α-tubulin and its stable form, acetylated α-tubulin, were not affected by SPAG-1 RNAi (Figure 5D and Supplemental Figure S3).

To illuminate the underlying mechanism for defective spindle morphogenesis in SPAG-1–silenced oocytes, we examined γ-tubulin, a well-recognized MTOC-associated protein regulating spindle morphogenesis. In control MI oocytes, γ-tubulin canonically

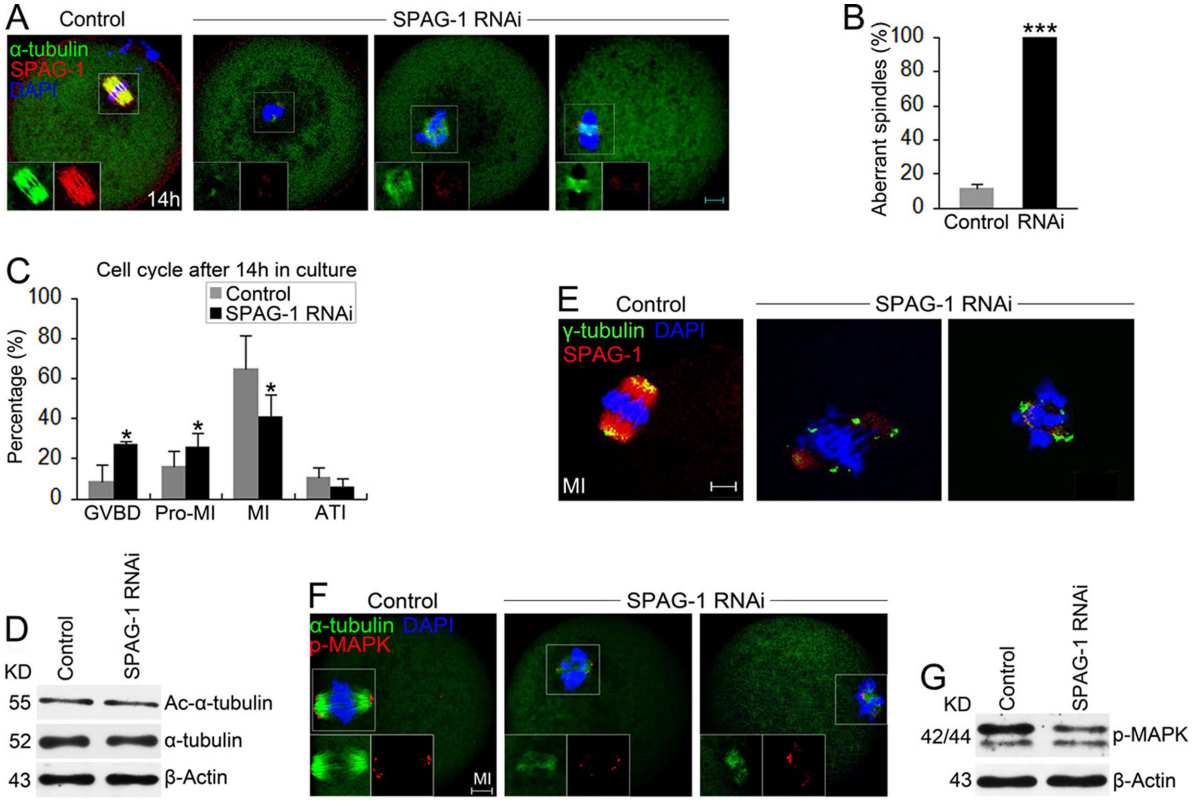

FIGURE 5: SPAG-1 is required for meiotic spindle morphogenesis and MAPK phosphorylation. Oocytes silenced with control siRNA or SPAG-1 siRNA were lysed for IB or continuously cultured for cell cycle or immunofluorescence analysis. (A) Spindle morphology in SPAG-1–depleted oocytes after 14 h in culture. SPAG-1, red; α-tubulin, green; DAPI, blue. Note that most SPAG-1–silenced oocytes failed to execute first polar body extrusion, showing various morphologically defective and even exterminated spindles. Three representative examples of SPAG-1–silenced oocytes are shown. (B) Rate of aberrant spindles in control ($n = 52$) oocytes and SPAG-1 RNAi ($n = 19$) oocytes. (C) Cell cycle analysis of unmatured oocytes in control ($n = 137$) and SPAG-1 RNAi groups ($n = 129$) based on the spindle and chromosome morphologies after 14 h in culture. (D) IB of acetylated-α-tubulin and α-tubulin in oocytes. (E) Representative images of MI oocytes stained with anti–γ-tubulin (green), SPAG-1 (red) antibodies, and DAPI (blue). γ-Tubulin displayed various mislocalizations in SPAG-1 RNAi oocytes instead of being concentrated on spindle poles as in control oocytes. Regions of spindle and chromosomes are magnified. (F) Confocal *Z*-projections of MI oocytes stained with anti–p-MAPK (red), SPAG-1 (green) antibodies, and DAPI (blue). Of note, p-MAPK in control oocytes appeared at the spindle poles; conversely, disrupted localization and decreased abundance of p-MAPK were detected in SPAG-1–silenced oocytes. (G) Expression of phosphorylated MAPK in oocytes. Enlargements correspond to the highlighted regions shown inside the merged images. Data are presented as mean ± SEM. $*p < 0.05$ and $***p < 0.001$. Scale bar, 10 μm.

localized at the spindle poles. Conversely, SPAG-1 silencing markedly disrupted the localization of γ-tubulin: γ-tubulin detached from spindle poles and scattered around the chromosomes (Figure 5E). γ-Tubulin alone is not sufficient for sustaining spindle assembly without the concerted action of additional regulators, including phospho-MAPK, which facilitates the recruitment or activation of microtubule nucleators to MTOCs, and SPAG-1 has been implicated in the MAPK pathway. To this end, we further studied phospho-MAPK. Of note, in striking contrast to control MI oocytes, in which phospho-MAPK localized at the spindle poles, the localization of phospho-MAPK in SPAG-1–depleted oocytes was distorted, with diminished or dispersed signals around spindles (Figure 5F). In addition, the ablated phosphorylation of MAPK by SPAG-1 silencing was confirmed by immunoblot (IB; Figure 5G). Taking the results together shows that SPAG-1 depletion induces the spindle morphogenesis defect by interfering with phosphorylation of MAPK and its subsequent localization.

SPAG-1 RNAi disrupts CGFD formation and actin filament assembly

To further understand the polar body extrusion defect elicited by SPAG-1 depletion, we examined actin cap and CGFD formation, which are essential for oocyte polarization, and disruption of which usually causes failure in cytokinesis. After 8 h in culture, cortical granules redistributed to form CGFD and actin reassembled to form an actin cap in control oocytes. In sharp contrast, neither CGFD nor the actin cap was present in SPAG-1–silenced oocytes (Figure 6, A and B). More importantly, the F-actin around the spindle midbody (contractile ring) was observed in control oocytes proceeding to the anaphase I (AI) stage, whereas the contractile ring was not assembled but disappeared in SPAG-1–deleted oocytes (Figure 6B) In addition, actin expression, as revealed by immunofluorescence analysis, abruptly decreased (Figure 6C). To uncover the underlying mechanism of the disrupted actin dynamic, we studied the PKC-CDC42-N-WASP-Arp2/3 axis, the activity of which in cortex remodeling has

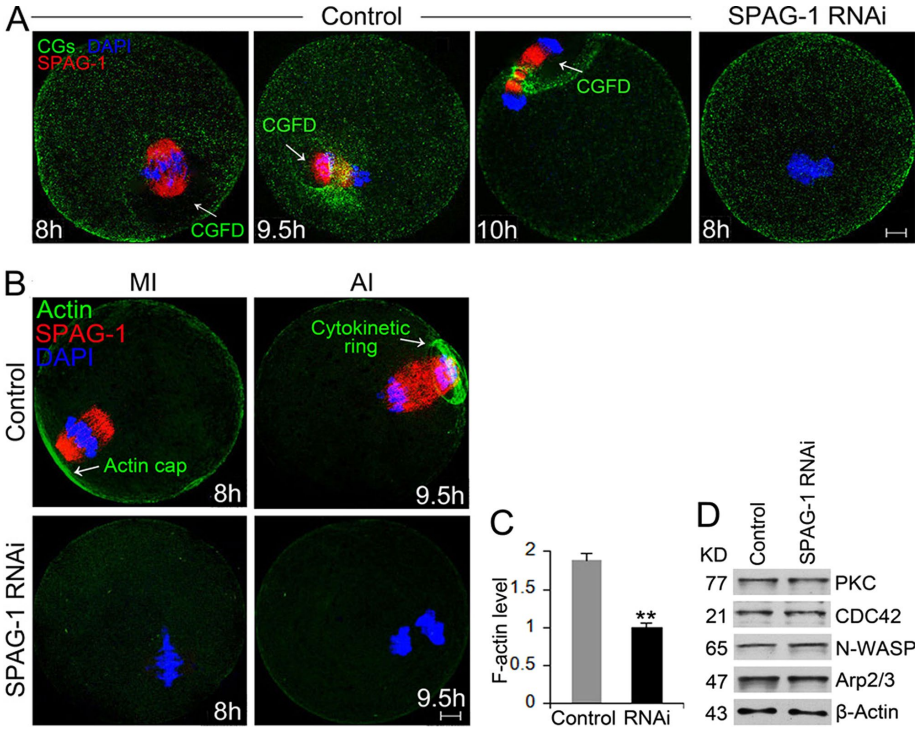

FIGURE 6: SPAG-1 RNAi disrupts the CGFD and actin cap formation. Formation of CGFD (A) and actin caps (B) in oocytes stained for SPAG-1 (red) and lectin (green, CGFD) or phalloidin (green, F-actin). DNA was labeled with DAPI (blue). The chromosomes migrated to cortex, and subsequent cortical reorganization occurred from the MI stage in control oocytes, whereas no CGFD, actin caps, or contractile ring was observed in SPAG-1–silenced oocytes. Scale bar, 10 μm. (C) Quantification of relative fluorescence intensity of F-actin in B. (D) IB analysis of actin-related regulators. $^{**}p < 0.01$. Scale bar, 10 μm.

been demonstrated (Dehapiot *et al.*, 2013; Humphries *et al.*, 2014; Kotak *et al.*, 2014; Wang *et al.*, 2014). However, the signaling pathway appeared to be unaffected by SPAG-1 depletion (Figure 6C). Overall, these data show that cortex remodeling is disrupted in SPAG-1–depleted oocytes, indicative of the failure of cytokinetic abscission and subsequent polar body emission.

The SAC is functional in the absence of SPAG-1

Inability to complete meiosis I division might be due to the activation of the SAC by defective spindle morphogenesis (Kouznetsova *et al.*, 2007). Therefore we determined BubR1, a principal component of SAC in oocytes, after 4.5 and 10 h in culture, the time points at which oocytes proceed to pro-MI and anaphase/telophase I, respectively. The BubR1 signals at kinetochores were comparable in both groups at the pro-MI stage. When oocytes entered into the anaphase/telophase I phase, homologous chromosomes segregated, and the kinetochore-localized BubR1 disappeared in control oocytes. However, in SPAG-1–depleted oocytes, the homologous chromosomes failed to segregate, and BubR1 signals persisted at kinetochores (Figure 7A). Moreover, BubR1 expression was indistinguishable in the two groups (Figure 7B), further confirming that SAC is functional in SPAG-1–silenced oocytes to keep meiosis in check.

DISCUSSION

Characterizing the error-prone journey through oocyte meiotic division to generate a haploid egg is challenging and is of great significance for female fertility. In this study, we find, for the first time, to our knowledge, a novel role of SPAG-1 in mammalian oogenesis. Our data indicate that SPAG-1 interferes with energy metabolism, MAPK phosphorylation, and cortex remodeling to orchestrate meiotic resumption and cytoskeleton architecture in mouse oocytes (Figure 8). This can broaden our understanding of molecular mechanisms of human infertility and subfertility.

SPAG-1 has pivotal roles in meiotic resumption and polar body extrusion

To delineate the relevance of SPAG-1 in meiotic program, we first studied the localization and expression patterns of SPAG-1 during oocyte meiotic progression. Immunofluorescence analysis showed a microtubule-associated dynamic of SPAG-1 during both in vivo and in vitro meiotic progression, which was confirmed by nocodazole treatment, and the expression profile of SPAG-1 during oocyte meiosis is consistent with the oocyte proteomic study (Wang *et al.*, 2010). The observation of similar SPAG-1 signals in in vivo– and in vitro–analyzed GV oocytes soon before GVBD deciphered the discrepancy in immunostaining signals of SPAG-1 seen during GV oocytes between in vivo and in vitro oocytes prepared at different developmental stages. After silencing of SPAG-1, a precipitous decline instead of a block in polar body extrusion is induced because of the inefficient depletion of SPAG-1 expression in all oocytes (unpublished data). In addition, the impaired GVBD after SPAG-1 depletion is found at a series of time points and further supported by the presence of >60% of oocytes at the GV stage even after 14 h in culture. Therefore we propose that SPAG-1 is an important regulator of mammalian oocyte meiotic progression.

SPAG-1 interferes with energy homeostasis in mouse oocytes

One striking phenotype in our study is the impaired kinetics of GVBD. Mammalian oocytes require a precise regulation of energy metabolism to sustain highly energy dependent meiotic events, including GVBD. Dysfunction of mitochondrial dynamics, which subsequently disrupts cell energy homeostasis, has been implicated in compromised developmental competence in oocytes (Gu *et al.*, 2015; Wu *et al.*, 2015). AMPK serves as the cell energy sensor, and its activity is potently stimulated by an increase in AMP level; it is fully activated by phosphorylation. The maintenance of energy balance by AMPK activation is accomplished by simultaneously stimulating ATP production and inhibiting ATP-consuming processes (Chen *et al.*, 2009; Ya and Downs, 2013; Hurtado de Llera *et al.*, 2015). In SPAG-1–silenced oocytes, the energy homeostasis is disrupted, as evidenced by a robust reduction in ATP production, an elevation of AMP level, as indicated by activation of AMPK, and an appreciable increase in cAMP concentration, which suppresses oocyte meiotic resumption. Significantly, the ATP-consuming processes—for example, phosphorylation of cyclin B1 and MAPK—are attenuated. It is well known that a boost in AMPK activation induces meiotic resumption in mouse oocyte and is likewise required for mitotic entry in mitotic cells (Chen *et al.*, 2009; Mao *et al.*, 2013; Ya and Downs, 2013), which deviates from the observations in our

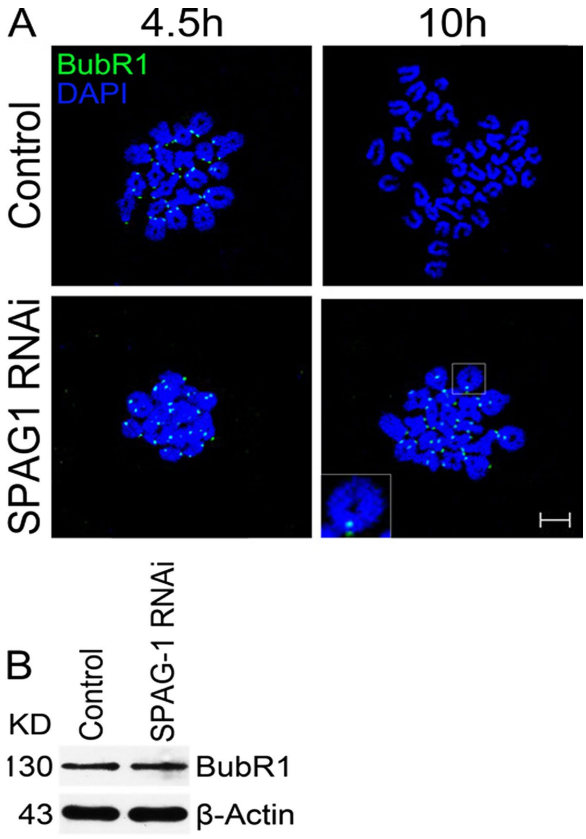

FIGURE 7: The spindle assembly checkpoint is functional in the absence of SPAG-1. (A) Chromosome spreading analysis of BubR1. Live GV oocytes silenced with control siRNA or SPAG-1 siRNA were cultured in M16 medium for 4.5 and 10 h, corresponding to pro-MI and AI stages, respectively, followed by chromosome spreading. BubR1, green; DNA, blue. Scale bar, 10 μm. (B) Immunoblot of BubR1 in GV oocytes.

study. This difference might be due to the fact that the relevance of AMPK activity in meiotic resumption was previously demonstrated by genetic interruption or chemical disruption without alteration of energy homeostasis, whereas in our study, activation of AMPK might be a consequence of disrupted energy homeostasis. Thus the effect of AMPK activity on GVBD might be because of a loss of ATP that is below the required threshold for development. Alternatively, AMPK targets different molecules under altered energy status during meiotic process to exert distinct roles. Moreover, AMPK has recently been found to elicit mitochondrial fragmentation when cells are under energy stress by acting on MFF, a mitochondrial fission factor that serves as an outer membrane receptor for Drp1 (Toyama *et al.*, 2016). Intriguingly, many mitochondrial biogenesis and dynamic regulators, including Drp1 and Mfn1/2, belong to the GTPase family (Son *et al.*, 2015; Yamamori *et al.*, 2015). Therefore whether GTPase SPAG-1 interferes with energy homeostasis in oocytes by triggering mitochondrial dysfunction deserves future investigation. In any case, our results are compelling evidence for interpreting, at least partially, the M-phase entry failure in SPAG-1–silenced oocytes.

SPAG-1 dictates spindle assembly and actin reorganization during mouse oocyte meiosis

Another relevant finding after SPAG-1 depletion is the cytoskeleton catastrophe. The mammalian oocyte is devoid of centrosomes and thus of associated astral microtubules, and thus the nucleation and organization of bipolar spindles in mammal oocytes is conferred MTOCs (Schuh and Ellenberg, 2007; Lane *et al.*, 2012; Han *et al.*, 2015). In our study, defective spindle morphogenesis is incurred in SPAG-1–silenced oocytes because microtubules completely fail to assemble. Furthermore, γ-tubulin, a well-established MTOC-associated protein that is instrumental for spindle morphogenesis, is mislocalized. Of note, the recruitment of γ-tubulin to spindle poles requires the concerted actions of additional regulators, including phospho-MAPK, whose relevance in regulating meiotic spindle assembly in mouse oocytes has been demonstrated (Sun *et al.*, 2011; Zhang *et al.*, 2015). In line with this notion, both phosphorylation of MAPK and accumulation of phospho-MAPK to spindle poles are attenuated, causally linking the dysfunction of phospho-MAPK to γ-tubulin mislocalization and aberrant spindle assembly.

Oocyte meiotic divisions are extremely asymmetric, which highlights the significance of cortical reorganization to achieve polarization. Of note, the attenuated actin dynamics in SPAG-1–silenced oocytes appears unlikely to be explained by the PKC-CDC42-N-WASP-Arp2/3 axis, the pivotal roles of which in actin polymerization have been documented by a wealth of studies. The finding that the Cdc42/N-WASP pathway is dispensable for first polar emission further supports our hypothesis (Dehapiot *et al.*, 2013). It is worth noting that the effect of SPAG-1 depletion on the subcellular localization of components from this pathway remains an interesting issue.

Significantly, AMPK is proposed to have dual roles of cell structure regulation and energy sensing. Either increase or decrease of AMPK away from the physiological set point negatively modified motility and membrane reorganization in boar spermatozoa (Hurtado de Llera *et al.*, 2015). AMPK was reported to associate with multiple mitotic structures, including spindle poles and cleavage furrow, and disruption of AMPK educes chromosomal segregation and cytokinesis defects (Vazquez-Martin *et al.*, 2013; Ya and Downs, 2013). Whether the defects in spindle morphogenesis and cortical architecture could be shared by the altered AMPK activity in SPAG-1–silenced oocytes deserves further exploration. Similarly, MAPK is involved in a spectrum of cell cycle processes, and abrogation of MAPK1/2 phosphorylation decreases F-actin in epithelial cells (Kutsuna *et al.*, 2004), raising the possibility that the ablated MAPK phosphorylation contributes to the disrupted actin dynamic in SPAG-1–silenced oocytes.

In conclusion, our study shows that SPAG-1 helps to guarantee the proper execution of the meiotic program, opposing chromosomal missegregation and preventing aneuploidy in mammalian oocytes.

MATERIALS AND METHODS

Animal studies

The present study used wild-type Kunming strain (KM) mice. Animals were obtained from the local Central Animal Laboratory and housed in the experimental animal center of Huazhong Agricultural University under a 12 h light/12 h dark regimen at a temperature of 22°C with water and food ad libitum. The study was conducted with the approval of the Ethical Committee of the Hubei Research Center of Experimental Animals (Approval ID: SCXK [Hubei] 20080005), and all experimental procedures were performed in accordance with the guidelines of the Committee of the Animal Research Institute, Huazhong Agricultural University, China.

Antibodies and reagents

Goat anti-SPAG-1 polyclonal antibody (98146) and mouse anti–γ-tubulin monoclonal antibody (17787) were purchased from

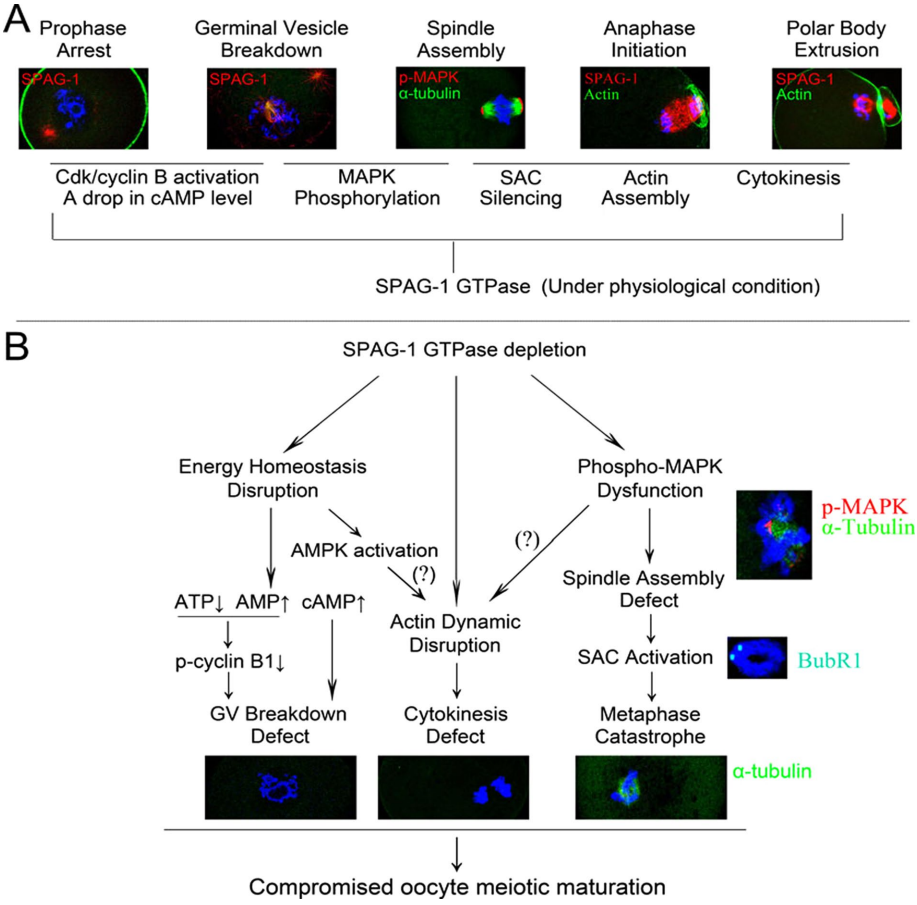

FIGURE 8: Key functions of SPAG-1 in mouse oocyte meiotic program under physiological and depleted conditions.

Santa Cruz Biotechnology (Santa Cruz, CA); rabbit anti–phospho-p44/42 MAPK monoclonal antibody (4370) and rabbit anti–phospho-cyclin B1 polyclonal antibody (4131) were purchased from Cell Signaling Technology (Danvers, MA); rabbit anti–phospho-AMPKα monoclonal antibody (133448), sheep anti-BubR1 polyclonal antibody (28193) and rabbit anti–histone H3 (acetyl K9) polyclonal antibody (10812) were obtained from Abcam (Cambridge, United Kingdom); mouse monoclonal anti–fluorescein isothiocyanate (FITC)-α-tubulin antibody (F2168) was produced by Sigma-Aldrich (St. Louis, MO). FITC-conjugated donkey anti-sheep immunoglobulin G (IgG) (H+L) was obtained from Jackson ImmunoResearch Laboratories (West Grove, PA).

FITC-phalloidin (P5282) and FITC-lectin (L7381) were purchased from Sigma-Aldrich. Unless otherwise specifically stated, all other reagents were obtained from Sigma-Aldrich.

Follicles, zygotes, and early-embryo collection

Primordial, primary, secondary, and antral follicles were isolated from the ovaries of 1-, 3-, 12-, and 21-d-old mice, respectively.

To analyze meiosis II progression and early embryogenesis (zygotic divisions), 9- to 10- wk-old female mice were mated after superovulation by applying 10 IU of pregnant mare serum gonadotropin (PMSG) and 10 IU of human chorionic gonadotropin (HCG) with an interval of 48 h. Meiosis of MII stage–arrested oocytes was reinitiated by fertilization, and fertilized oocytes were collected from the oviducts of mated females approximately at 40 min to 20 h after the appearance of the vaginal plug. Pronuclear- and one-cell-stage embryos were collected 20–22 h after hCG treatment, and two-, four-, and eight-cell- and blastocyst-stage embryos were harvested 46–47, 50–52, 68–70, and 116–118 h after hCG application, respectively.

All collection procedures were conducted in prewarmed M2 medium, and the samples were prepared for further analysis.

Oocyte retrieval and culture

To study in vivo oocyte meiotic maturation, female mice at the age of 3–4 wk were superovulated by the aforementioned procedure. Ovaries were dissected at hourly intervals from the mice at 4–10 h after hCG injection. Cumulus cells surrounding oocytes were then harvested, and denuded oocytes were obtained by exposing oocytes in prewarmed (37°C) M2 medium containing hyaluronidase (0.3 mg/ml) with gentle pipetting.

To analyze in vitro oocyte meiotic maturation, ovaries were dissected from 3- to 4- wk-old mice, and oocytes were harvested in prewarmed M2 medium containing 50 μM 3-isobutyl-1-methylxanthine (IBXM) to prevent meiosis resumption. To induce meiotic maturation, oocytes were washed out of IBXM and released into fresh M16 medium at 37°C and 5% CO_2 in air for 0, 2, 4.5, 8, 9.5, and 14 h, corresponding to GV, GVBD, pro-MI, MI, AI, and MII stages, respectively. Oocytes at specific stages were collected according to the experimental purpose.

Spindle perturbation drug treatment

Nocodazole was prepared as 10 mg/ml in dimethyl sulfoxide (DMSO) stock (–20°C) and diluted in M16 medium to a working concentration of 20 μg/ml. For microtubule depolymerization, wild-type MI or MII oocytes were incubated with nocodazole for 15 min, followed by immunostaining of SPAG-1 and α-tubulin. For microtubule reassembly, after nocodazole treatment, oocytes were washed thoroughly and recovered in fresh M16 medium for 30 min, followed by immunofluorescence analysis. All control oocytes were maintained in M16 medium containing DMSO at the same concentration.

Immunofluorescence and confocal microscopy

Immunofluorescence and confocal assays were preformed as previously described (Huang *et al.*, 2015). For immunolabeling, the following primary antibodies and dilutions were used: goat anti–SPAG-1 antibody (1:50), mouse anti–γ-tubulin antibody (1:100), rabbit anti–phospho-p44/42 MAPK antibody (1:100), rabbit anti–acetylated-α-tubulin (1:100), and FITC-labeled mouse anti–α-tubulin (1:100). FITC- or Cy3-labeled goat anti-rabbit or goat anti-mouse (1:100; Boster, Pleasanton, CA) antibodies were used as the secondary antibodies. F-actin and cortical granules were labeled with FITC-phalloidin (1:100) and FITC-lectin (1:100), respectively. For negative control, the primary antibody was replaced by rabbit IgG.

Microinjection of small interfering RNA oligonucleotides

For microinjection, GV-stage oocytes were collected in M2 medium supplemented with 50 μM IBXM. After 2 h of recovery, 5–10 pl of

30 μM control small interfering RNA (siRNA; sc-37007; Santa Cruz Biotechnology) or SPAG-1 siRNA (sc-153701; Santa Cruz Biotechnology) was injected into the cytoplasm of oocytes. After microinjection, oocytes were incubated in M2 medium containing 50 μM IBXM for 24 h to achieve efficient SPAG-1 knockdown. Oocytes were immediately collected for analysis or thoroughly washed out of IBXM and cultured in M16 medium for in vitro meiotic maturation.

ATP and cAMP assessment

Four groups of 30 control or SPAG-1–depleted oocytes were retrieved for ATP and cAMP assessment. ATP and cAMP relative concentrations were evaluated by using the Cell-Titer-Glo ATP Assay (Promega, Madison, WI) and cAMP-Glo Assay (Promega), respectively, according to the manufacturer's instructions. Of note, the cAMP assay is based on the principle that cAMP stimulates protein kinase A holoenzyme activity, decreasing available ATP and leading to decreased luminescence intensity in a coupled luciferase reaction. Thus, elevated cAMP abundance is indirectly revealed by decreased luminescence intensity of ATP.

Chromosome spreading

For BubR1 analysis, chromosome spreading was performed as previously described (Huang *et al.*, 2015).

Immunoblotting

About 300 oocytes of each group were briefly washed in phosphate-buffered saline and then lysed in 2× SDS buffer and stored at −80°C until use. Immunoblot analysis was preformed as described (Huang *et al.*, 2015). For immunolabeling, the following primary antibodies and dilutions were used: goat anti–SPAG-1 antibody (1:200), anti–phospho-AMPKα antibody (1:1500), anti–phospho-cyclin B1 antibody (1:1000), anti–histone H3 (acetyl K9) antibody (1:1000), rabbit anti–cyclin B2 polyclonal antibody (1:200; Santa Cruz Biotechnology), rabbit anti–α-tubulin monoclonal antibody (1:1000; Cell Signaling Technology), rabbit anti–acetylated-α-tubulin (1:1000; Cell Signaling Technology), anti–phospho-H2A.X antibody (1:1000; Cell Signaling Technology), rabbit anti–phospho-p44/42 MAPK antibody (1:1000), rabbit anti-PKC monoclonal antibody (1:1000; Abcam), anti-CDC42 antibody (1:1000; Abcam), anti–N-WSAP antibody (1:1000; Abcam), anti-Arp3 antibody (1:1000; Abcam), and anti-BubR1 antibody (1:1000). The data were normalized to β-actin.

Statistical analysis

Data are mean ± SEM from three duplicated assays and are analyzed by a paired-sample *t* test with SPSS software (SPSS, Chicago, IL); $p < 0.05$ is set as statistically significant. Statistical difference is indicated by different superscripts. The number of oocytes collected is given as *n* in parentheses.

ACKNOWLEDGMENTS

This study was supported by the National Natural Science Foundation of China (Grants No. 31071273 and 31171378) and the Fundamental Research Funds for the Central Universities (Program NO. 2014PY045). C.J.H. gratefully acknowledges technical support from the State Key Laboratory of Agricultural Microbiology, Huazhong Agricultural University.

REFERENCES

Almonacid M, Terret ME, Verlhac MH (2014). Actin-based spindle positioning: new insights from female gametes. J Cell Sci 127, 477–483.

Chen J, Chi MM, Moley KH, Downs SM (2009). cAMP pulsing of denudes mouse oocytes increases meiotic resumption via activation of AMP-activated protein kinase. Reproduction 138, 759–770.

Clarke PR, Zhang C (2001). Ran GTPase: a master regulator of nuclear structure and function during the eukaryotic cell division cycle? Trends Cell Biol 11, 366–371.

Clift D, Schuh M (2015). A three-step MTOC fragmentation mechanism facilitates bipolar spindle assembly in mouse oocytes. Nat Commun 6, 7217.

Dehapiot B, Carrière V, Carroll J, Halet G (2013). Polarized Cdc42 activation promotes polar body protrusion and asymmetric division in mouse oocytes. Dev Biol 377, 202–212.

Deng M, Suraneni P, Schultz RM, Li R (2007). The Ran GTPase mediates chromatin signaling to control cortical polarity during polar body extrusion in mouse oocytes. Dev Cell 12, 301–308.

Dumont J, Desai A (2012). Acentrosomal spindle assembly and chromosome segregation during oocyte meiosis. Trends Cell Biol 22, 241–249.

Gui L, Homer H (2013). Hec1-dependent cyclin B2 stabilization regulates the G2-M transition and early prometaphase in mouse oocytes. Dev Cell 25, 43–54.

Gu L, Liu H, Gu X, Boots C, Moley KH, Wang Q (2015). Metabolic control of oocyte development: linking maternal nutrition and reproductive outcomes. Cell Mol Life Sci 72, 251–271.

Han L, Ge J, Zhang L, Ma R, Hou X, Li B, Moley K, Wang Q (2015). Sirt6 depletion causes spindle defects and chromosome misalignment during meiosis of mouse oocyte. Sci Rep 5, 15366.

Holt JE, Lane SI, Jones KT (2013). The control of meiotic maturation in mammalian oocytes. Curr Top Dev Biol 102, 207–226.

Holubcová Z, Blayney M, Elder K, Schuh M (2015). Human oocytes. Error-prone chromosome-mediated spindle assembly favors chromosome segregation defects in human oocytes. Science 348, 1143–1147.

Huang CJ, Wu D, Khan AF, Huo LJ (2015). The SUMO protease SENP3 orchestrates G2-M transition and spindle assembly in mouse oocytes. Sci Rep 5, 15600.

Humphries AC, Donnelly SK, Way M (2014). Cdc42 and the Rho GEF intersectin-1 collaborate with Nck to promote N-WASP-dependent actin polymerisation. J Cell Sci 127, 673–685.

Hurtado de Llera A, Martin-Hidalgo D, Gil MC, Garcia-Marin LJ, Bragado MJ (2015). Cdc42 and the Rho GEF intersectin-1 collaborate with Nck to promote N-WASP-dependent actin polymerisation. J Cell Sci 127, 673–685.

Knowles MR, Ostrowski LE, Loges NT, Hurd T, Leigh MW, Huang L, Wolf WE, Carson JL, Hazucha MJ, Yin W, *et al.* (2013). Mutations in SPAG1 cause primary ciliary dyskinesia associated with defective outer and inner dynein arms. Am J Hum Genet 93, 711–720.

Kotak S, Busso C, Gonczy P (2014). NuMA interacts with phosphoinositides and links the mitotic spindle with the plasma membrane. EMBO J 33, 1815–1830.

Kouznetsova A, Lister L, Nordenskjöld M, Herbert M, Höög C (2007). Bi-orientation of achiasmatic chromosomes in meiosis I oocytes contributes to aneuploidy in mice. Nat Genet 39, 186–188.

Kutsuna H, Suzuki K, Kamata N, Kato T, Hato F, Mizuno K, Kobayashi H, Ishii M, Kitagawa S (2004). Actin reorganization and morphological changes in human neutrophils stimulated by TNF, GM-CSF, and G-CSF: the role of MAP kinases. Am J Physiol Cell Physiol 286, C55–C64.

Lane SI, Yun Y, Jones KT (2012). Timing of anaphase-promoting complex activation in mouse oocytes is predicted by microtubule-kinetochore attachment but not by bivalent alignment or tension. Development 139, 1947–1955.

Lin W, Zhou X, Zhang M, Li Y, Miao S, Wang L, Zong S, Koide SS (2001). Expression and function of the HSD-3.8 gene encoding a testis-specific protein. Mol Hum Reprod 7, 811–818.

Liu N, Qiao Y, Cai C, Lin W, Zhang J, Miao S, Zong S, Koide SS, Wang L (2006). A sperm component, HSD-3.8 (SPAG1), interacts with G-protein beta 1 subunit and activates extracellular signal-regulated kinases (ERK). Front Biosci 11, 1679–1689.

Mao L, Li N, Guo Y, Xu X, Gao L, Xu Y, Zhou L, Liu W (2013). AMPK phosphorylates GBF1 for mitotic Golgi disassembly. J Cell Sci 126, 1498–1505.

Nagaoka SI, Hassold TJ, Hunt PA (2012). Human aneuploidy: mechanisms and new insights into an age-old problem. Nat Rev Genet 13, 493–504.

Neesse A, Gangeswaran R, Luettges J, Feakins R, Weeks ME, Lemoine NR, Crnogorac-Jurcevic T (2007). Sperm-associated antigen 1 is expressed early in pancreatic tumorigenesis and promotes motility of cancer cells. Oncogene 26, 1533–1545.

Pfender S, Kuznetsov V, Pasternak M, Tischer T, Santhanam B, Schuh M (2015). Live imaging RNAi screen reveals genes essential for meiosis in mammalian oocytes. Nature 524, 239–242.

Qiao J, Li R (2014). Fertility preservation: challenges and opportunities. Lancet 384, 1246–1247.

Saloojee H, Coovadia H (2015). Maternal age matters: for a lifetime, or longer. Lancet Global Health 3, e342–e343.
Schuh M, Ellenberg J (2007). Self-organization of MTOCs replaces centrosome function during acentrosomal spindle assembly in live mouse oocytes. Cell 130, 484–498.
Serio G, Margaria V, Jensen S, Oldani A, Bartek J, Bussolino F, Lanzetti L (2011). Small GTPase Rab5 participates in chromosome congression and regulates localization of the centromere-associated protein CENP-F to kinetochores. Proc Natl Acad Sci USA 108, 17337–17342.
Son MJ, Kwon Y, Son MY, Seol B, Choi HS, Ryu SW, Choi C, Cho YS (2015). Mitofusins deficiency elicits mitochondrial metabolic reprogramming to pluripotency. Cell Death Differ 22, 1957–1969.
Sun SC, Xu YN, Li YH, Lee SE, Jin YX, Cui XS, Kim NH (2011). WAVE2 regulates meiotic spindle stability, peripheral positioning and polar body emission in mouse oocytes. Cell Cycle 10, 1853–1860.
Toyama EQ, Herzig S, Courchet J, Lewis TL Jr, Losón OC, Hellberg K, Young NP, Chen H, Polleux F, Chan DC (2016). Metabolism. AMP-activated protein kinase mediates mitochondrial fission in response to energy stress. Science 351, 275–281.
Vazquez-Martin A, Corominas-Faja B, Oliveras-Ferraros C, Cufí S, Dalla Venezia N, Menendez JA (2013). Serine79-phosphorylated acetyl-CoA carboxylase, a downstream target of AMPK, localizes to the mitotic spindle poles and the cytokinesis furrow. Cell Cycle 12, 1639–1641.
Wang F, Zhang L, Zhang GL, Wang ZB, Cui XS, Kim NH, Sun SC (2014). WASH complex regulates Arp2/3 complex for actin-based polar body extrusion in mouse oocytes. Sci Rep 4, 5596.
Wang S, Kou Z, Jing Z, Zhang Y, Guo X, Dong M, Wilmut I, Gao S (2010). Proteome of mouse oocytes at different developmental stages. Proc Natl Acad Sci USA 107, 17639–17644.
Wang Y, Teng Z, Li G, Mu X, Wang Z, Feng L, Niu W, Huang K, Xiang X, Wang C (2015). Cyclic AMP in oocytes controls meiotic prophase I and primordial folliculogenesis in the perinatal mouse ovary. Development 142, 343–351.
Wu LL, Russell DL, Wong SL, Chen M, Tsai TS, St John JC, Norman RJ, Febbraio MA, Carroll J, Robker RL (2015). Mitochondrial dysfunction in oocytes of obese mothers: transmission to offspring and reversal by pharmacological endoplasmic reticulum stress inhibitors. Development 142, 681–691.
Ya R, Downs SM (2013). Suppression of chemically induced and spontaneous mouse oocyte activation by AMP-activated protein kinase. Biol Reprod 88, 70.
Yamamori T, Ike S, Bo T, Sasagawa T, Sakai Y, Suzuki M, Yamamoto K, Nagane M, Yasui H, Inanami O (2015). Inhibition of the mitochondrial fission protein dynamin-related protein 1 (Drp1) impairs mitochondrial fission and mitotic catastrophe after x-irradiation. Mol Biol Cell 26, 4607–4617.
Yi K, Unruh JR, Deng M, Slaughter BD, Rubinstein B, Li R (2011). Dynamic maintenance of asymmetric meiotic spindle position through Arp2/3-complex-driven cytoplasmic streaming in mouse oocytes. Nat Cell Biol 13, 1252–1258.
Yu C, Zhang YL, Pan WW, Li XM, Wang ZW, Ge ZJ, Zhou JJ, Cang Y, Tong C, Sun QY, Fan HY (2013). CRL4 complex regulates mammalian oocyte survival and reprogramming by activation of TET proteins. Science 342, 1518–1521.
Yun Y, Lane SI, Jones KT (2014). Premature dyad separation in meiosis II is the major segregation error with maternal age in mouse oocytes. Development 141, 199–208.
Zhang M, Xia G (2012). Hormonal control of mammalian oocyte meiosis at diplotene stage. Cell Mol Life Sci 69, 1279–1288.
Zhang Y, Wang F, Niu YJ, Liu HL, Rui R, Cui XS, Kim NH, Sun SC (2015). Formin mDia1, a downstream molecule of FMNL1, regulates Profilin1 for actin assembly and spindle organization during mouse oocyte meiosis. Biochim Biophys Acta 1853, 317–327.